Data analysis of continuous gravitational wave: Fourier transform-I

D.C. Srivastava[1,2*] and S.K. Sahay[1‡]

[1]Department of Physics, DDU Gorakhpur University, Gorakhpur-273009, U.P., India.

[2]Visiting Associate, Inter University Centre for Astronomy and Astrophysics, Post Bag 4, Ganeshkhind, Pune-411007, India.

Abstract

We present the Fourier Transform of a continuous gravitational wave. We have analysed the data set for one day observation time and our analysis is applicable for arbitrary location of detector and source. We have taken into account the effects arising due to rotational as well as orbital motions of the earth.

1 Introduction

The first generation of long-baseline laser interferometers and ultra cryogenic bar detectors will start collecting data very soon. The network of detectors is expected not only to confirm the existence of gravitational waves (GW) but will also provide the information about the structure and the dynamics of its source. At the present stage, the data analysis depends largely upon the study of the expected characteristic of its potential sources and the waveforms. Majority of the experimental searches is focused on the detection of burst and *chirp* signals. However, the interest in the data analysis for continuous gravitational wave (CGW) signals is growing. A prime example of sources of this type is a spinning neutron star. Many research groups around the globe are working extensively on the data analysis for spinning neutron stars (Jaranwoski, et.al 1998, 1999, 2000; Brady et. al. 1998, 2000; Królak 1999).

*e-mail: dcsrivastava@now-india.com

†e-mail: ssahay@iucaa.ernet.in

‡Present address: Inter University Centre for Astronomy and Astrophysics, Post Bag 4, Ganeshkhind, Pune - 411007, India

The detection of GW signals in the noisy output of the detectors has its own problems, not the least of which is the sheer volume of data analysis. Bar detectors have essentially the same problems as interferometers in reference to CGW sources. Each detector produces a single data stream that may contain many kinds of signals. Detectors don't point, but rather sweep their broad quadrupolar beam pattern across the sky as the earth moves. So possible sources could be anywhere on the sky and accordingly the data analysis algorithms need to accommodate signals from any arbitrary location of its source.

In this and the subsequent paper we present analysis of Fourier Transform (FT) of the output data of a ground based laser interferometer. The output data has broad band noise and the signal is to be extracted out of it. For this, one has to enhance signal-to-noise ratio (SNR). This is achieved by analyzing long observation time data as SNR is directly proportional to the square root of observation time ($\sqrt{T_o}$). However, in a data for long duration, the monochromatic signal gets Doppler modulated due to (i) the orbital motions of the earth around the sun and (ii) the spin of the earth. The frequency modulation (FM) will spread the signal in a very large number of bins depending on the source location and the frequency. In addition to this, there is amplitude modulation (AM). As we will see in the sequel the amplitude of the detector output consists of simple harmonic terms with frequencies w_{rot} and $2w_{rot}$ where, w_{rot} stands for angular rotational frequency of the earth. Accordingly, the AM results in splitting of the FT into frequencies $\pm w_{rot}$ and $\pm 2w_{rot}$.

In the next section we present the noise free response of the laser interferometric detector and obtain the explicit beam pattern functions. In section 3 we discuss the Doppler effect and obtain Fourier transform (FT) of the FM signal for arbitrary source and detector locations taking into account the earth's rotational motion about its axis and its revolution around the sun. In section 4 the FT of the Doppler modulated complete response of the detector is obtained. Section 5 is the conclusion of the paper.

2 The noise free response of detector: Beam pattern and Amplitude modulation

Let a plane GW fall on a laser interferometer and produce changes in the arms of the detector. In order to express these changes quantitatively we have to specify the wave and the detector. Let XYZ and xyz represent respective frames characterising the wave and the detector. We assume the direction of propagation of the wave to be the Z axis and the vertical at the place of the detector to be the z axis. The difference of the changes δl in the arm lengths of the detector may be given via

$$R(t) = \frac{\delta l}{l_o} = -\sin 2\Omega \left[(\mathbf{A}_X^x \mathbf{A}_X^y - \mathbf{A}_Y^x \mathbf{A}_Y^y)\, h_+ + (\mathbf{A}_X^x \mathbf{A}_Y^y + \mathbf{A}_Y^x \mathbf{A}_X^y)\, h_\times \right] \tag{1}$$

where l_o is the normal length of the arms of the detector and 2Ω expresses the angle between them (Schutz and Tinto, 1987). The matrix $\left(\mathbf{A}_K^j\right)$ represents the transformation expressing the rotations to bring the wave frame (X, Y, Z) to the detector frame (x, y, z). The direction of the source may be expressed in any of the coordinates employed in Spherical Astronomy. However, we find it convenient to define it in Solar System Barycentre (SSB) frame, (X', Y', Z'). This SSB frame is nothing but astronomer's ecliptic coordinate system. Let θ and ϕ denote the celestial colatitude and celestial longitude of the source. These coordinates are related to the right ascension, $\bar{\alpha}$ and the declination, $\bar{\delta}$ of the source via

$$\left.\begin{aligned} \cos\theta &= \sin\bar{\delta}\cos\epsilon - \cos\bar{\delta}\sin\epsilon\sin\bar{\alpha} \\ \sin\theta\cos\phi &= \cos\bar{\delta}\cos\bar{\alpha} \\ \sin\theta\sin\phi &= \sin\bar{\delta}\sin\epsilon + \cos\bar{\delta}\cos\epsilon\sin\bar{\alpha} \end{aligned}\right\} \tag{2}$$

where ϵ represents obliquity of the ecliptic. We choose x axis as the bisector of the angle between the arms of the detector. At this stage the orientation of the detector in the horizontal plane is arbitrary. It is assigned with the help of the angle γ which the x axis makes with the local meridian. The location of the detector on the earth is characterised by the angles, α - colatitude and β - the local sidereal time, expressed in radians. The transformation matrix $\left(\mathbf{A}_K^j\right)$ may be expressed as

$$\mathbf{A} = \mathbf{DCB} \tag{3}$$

where
$\mathbf{B}$: rotation required to bring XYZ to $X'Y'Z'$
$\mathbf{C}$: rotation required to bring $X'Y'Z'$ to $x'y'z'$
$\mathbf{D}$: rotation required to bring $x'y'z'$ to xyz

Here $x'y'z'$ represents the frame associated with the earth. The Euler angles defining the corresponding rotation matrices are given via

$$\left.\begin{aligned} \mathbf{B} &: (\theta, \phi, \psi) \\ \mathbf{C} &: (0, \epsilon, 0) \\ \mathbf{D} &: (\alpha, \beta + \pi/2, \gamma - \pi/2) \end{aligned}\right\} \tag{4}$$

where ψ is a measure of the polarisation of the wave (Goldstein, 1980).
Let us write Eq. (1) as

$$R(t) = \frac{\delta l}{l_o} = -\sin 2\Omega \left[F_+ h_+ + F_\times h_\times\right] \tag{5}$$

The functions F_+ and $F_\times$ involve the angles $\theta, \phi, \psi, \epsilon, \alpha, \beta, \gamma$ and express the effect of the interaction of the wave and the detector. These are called antenna or beam patterns.

The explicit functional dependences of F_+ and $F_\times$ are given by Jotania and Dhurandhar (1994). It is pointed out that there are few minor errors in these expressions and these are later corrected by the authors in Jotania (1994). These functions appear complicated but may be written in simpler form by introducing following abbreviations.

$$\left.\begin{aligned} U &= \cos\alpha\cos\beta\cos\gamma - \sin\beta\sin\gamma\,, \\ V &= -\cos\alpha\cos\beta\sin\gamma - \sin\beta\cos\gamma\,, \\ X &= \cos\alpha\sin\beta\cos\gamma + \cos\beta\sin\gamma\,, \\ Y &= -\cos\alpha\sin\beta\sin\gamma + \cos\beta\cos\gamma \end{aligned}\right\} \tag{6}$$

$$\left.\begin{aligned} L &= \cos\psi\cos\phi - \cos\theta\sin\phi\sin\psi\,, \\ M &= \cos\psi\sin\phi + cos\theta\cos\phi\sin\psi\,, \\ N &= -\sin\psi\cos\phi - cos\theta\sin\phi\cos\psi\,, \\ P &= -\sin\psi\sin\phi + cos\theta\cos\phi\cos\psi\,, \\ Q &= \sin\theta\sin\phi\,, \qquad R = \sin\theta\cos\phi\,, \end{aligned}\right\} \tag{7}$$

$$\left.\begin{aligned} A &= 2XY\cos^2\epsilon - \sin^2\epsilon\sin^2\alpha\sin 2\gamma + \sin 2\epsilon(X\sin\alpha\sin\gamma - Y\sin\alpha\cos\gamma)\,, \\ B &= 2XY\sin^2\epsilon - \cos^2\epsilon\sin^2\alpha\sin 2\gamma - \sin 2\epsilon(X\sin\alpha\sin\gamma - Y\sin\alpha\cos\gamma)\,, \\ C &= \cos\epsilon(YU + XV) + \sin\epsilon(U\sin\alpha\sin\gamma - V\sin\alpha\cos\gamma)\,, \\ D &= -\sin\epsilon(YU + XV) + \cos\epsilon(U\sin\alpha\sin\gamma - V\sin\alpha\cos\gamma]\,, \\ E &= -2XY\cos\epsilon\sin\epsilon - \cos\epsilon\sin\epsilon\sin^2\alpha\sin 2\gamma + \cos 2\epsilon(X\sin\alpha\sin\gamma - Y\sin\alpha\cos\gamma) \end{aligned}\right\} \tag{8}$$

After straight-forward substitutions one obtains

$$\begin{aligned} F_+(t) &= \frac{1}{2}\left[2(L^2 - M^2)UV + (N^2 - P^2)A + (Q^2 - R^2)B\right] + (LN - MP)C \\ &\quad + (LQ + MR)D + (NQ + PR)E\,, \end{aligned} \tag{9}$$

$$\begin{aligned} F_\times(t) &= 2LMUV + NPA - \frac{1}{2}B\sin^2\theta\sin 2\phi + (LP + MN)C \\ &\quad + (MQ - LR)D + (PQ - NR)E \end{aligned} \tag{10}$$

The compactification obtained here arises due to the fact that above introduced abbreviations find places in the transformation matrices as follows

$$\mathbf{B} = \begin{pmatrix} L & N & Q \\ M & P & -R \\ \sin\theta\sin\psi & \sin\theta\cos\psi & \cos\theta \end{pmatrix} \tag{11}$$

$$\mathbf{C} = \begin{pmatrix} 1 & 0 & 0 \\ 0 & \cos\epsilon & \sin\epsilon \\ 0 & -\sin\epsilon & \cos\epsilon \end{pmatrix} \tag{12}$$

$$\mathbf{D} = \begin{pmatrix} U & V & \sin\alpha\cos\beta \\ X & Y & \sin\alpha\sin\beta \\ -\sin\alpha\cos\gamma & \sin\alpha\sin\gamma & \cos\alpha \end{pmatrix} \; ; \tag{13}$$

After algebraic manipulation Eqs. (9) and (10) may be expressed as

$$F_+(t) = F_{1_+}\cos 2\beta + F_{2_+}\sin 2\beta + F_{3_+}\cos\beta + F_{4_+}\sin\beta + F_{5_+} \; ; \tag{14}$$

$$F_\times(t) = F_{1_\times}\cos 2\beta + F_{2_\times}\sin 2\beta + F_{3_\times}\cos\beta + F_{4_\times}\sin\beta + F_{5_\times} \tag{15}$$

where F_{i_+} and $F_{i_\times}$ $(i = 1, 2, 3, 4, 5)$ are time independent expressions given via

$$\left.\begin{aligned} F_{1_+} &= -2G\cos\alpha\cos 2\gamma + \tfrac{H\sin 2\gamma}{2}(\cos^2\alpha + 1)\,, \\ F_{2_+} &= H\cos\alpha\cos 2\gamma + G\sin 2\gamma(\cos^2\alpha + 1)\,, \\ F_{3_+} &= I\sin\alpha\cos 2\gamma + J\sin 2\alpha\sin 2\gamma\,, \\ F_{4_+} &= 2J\sin\alpha\cos 2\gamma - \tfrac{I}{2}\sin 2\alpha\sin 2\gamma\,, \\ F_{5_+} &= \tfrac{3\sin^2\alpha\sin 2\gamma}{2}[H + L^2 - M^2]\,, \end{aligned}\right\} \; ; \tag{16}$$

$$\left.\begin{aligned} G &= \tfrac{1}{2}[(LQ + MR)\sin\epsilon - (LN - MP)\cos\epsilon]\,, \\ H &= \tfrac{1}{2}[(N^2 - P^2)\cos^2\epsilon - (L^2 - M^2) + (Q^2 - R^2)\sin^2\epsilon - (NQ + PR)\sin 2\epsilon]\,, \\ I &= \tfrac{1}{2}[(Q^2 - R^2)\sin 2\epsilon - (N^2 - P^2)\sin 2\epsilon - 2(NQ + PR)\cos 2\epsilon]\,, \\ J &= \tfrac{1}{2}[(LN - MP)\sin\epsilon + (LQ + MR)\cos\epsilon] \end{aligned}\right\} \tag{17}$$

Let us note that $F_{i_\times}$ is related to F_{i_+} via

$$F_{i_\times}(\theta,\phi,\psi,\alpha,\beta,\gamma,\epsilon) \;=\; F_{i_+}(\theta,\phi-\frac{\pi}{4},\psi,\alpha,\beta,\gamma,\epsilon)\;; \qquad i \;=\; 1,2,3,4,5 \tag{18}$$

This symmetry is representative of the quadrupolar nature of the detector and the wave. The detectors at different orientations will record different amplitudes in their responses. The explicit beam pattern functions may be computed easily for any instant of time. Due to the symmetries involved in F_+ and $F_\times$ it is sufficient to evaluate either of the beam patterns.

The amplitude modulation of the received signal is a direct consequence of the non-uniformity of the sensitivity pattern. As remarked earlier they are fairly complicated function of their arguments. Equations (14) and (15) reveal that the monochromatic signal frequency will split, due to AM, into five frequencies. This results in the distribution of energy in various frequencies and consequent reduction of the amplitude of the signal. The periodicity of the beam pattern F_+ and $F_\times$ with a period equal to one sidereal day is due to the diurnal motion of the Earth.

3 Doppler shift and Frequency modulation

The frequency of a monochromatic signal will be Doppler shifted due to the translatory motion of the detector acquired from the motions of the earth. Let us consider a CGW signal of constant frequency f_o. The frequency f' received at the instant t by the detector is given by

$$f'(t) = f_o\gamma_o\left(1+\frac{\mathbf{v}.\mathbf{n}}{c}(t)\right) \quad ; \quad \gamma_o = \left(1-\frac{v^2}{c^2}\right)^{-1/2} \tag{19}$$

where $\mathbf{n}$ is the unit vector from the antenna to the source, $\mathbf{v}$ is the relative velocity of the source and the antenna, and c is the velocity of light. The unit vector $\mathbf{n}$ from the antenna to the source, in view of the fact that the distance of the source is very large compared to the average distance of the centre of the SSB frame and the detector, may be taken parallel to the unit vector drawn from the centre of the SSB frame to the source. Hence,

$$\mathbf{n} \quad = \quad (\sin\theta\cos\phi \quad , \quad \sin\theta\sin\phi \quad , \quad \cos\theta) \tag{20}$$

As **v** keeps on changing continuously both in its amplitude and direction f' is a continuous function of t. Further, since $v \ll c$ we take $\gamma_o = 1$.

The radius vector $\mathbf{r}(t)$ in the SSB frame is given by (Kanti, et al. 1996)

$$\begin{aligned}\mathbf{r}(t) \;=\; & [R_{se}\cos(w_{orb}t) + R_e\sin\alpha\cos\beta \;,\; R_{se}\sin(w_{orb}t) + R_e\sin\alpha\sin\beta\cos\epsilon - \\ & R_e\cos\alpha\sin\epsilon\,, R_e\sin\alpha\sin\beta\sin\epsilon + R_e\cos\alpha\cos\epsilon]\;;\end{aligned} \tag{21}$$

$$\beta = \beta_o + w_{rot}t \tag{22}$$

where R_e, R_{se} and w_{orb} represent respectively the earth's radius, average distance between earth's centre from the origin of SSB frame and the orbital angular velocity of the earth. Here t represents the time in seconds elapsed from the instant the sun is at the Vernal Equinox and β_o is the local sidereal time at that instant. The Doppler shift is now given via

$$\begin{aligned}\frac{f'-f_o}{f_o} &= \frac{\mathbf{v}.\mathbf{n}}{c}(t) = \frac{\dot{\mathbf{r}}_\mathbf{t}.\mathbf{n}}{c} = \frac{R_{se}w_{orb}}{c}\sin\theta\sin(\phi - w_{orb}t) + \\ &\quad \frac{R_e w_{rot}}{c}\sin\alpha\left[\sin\theta\{\cos\beta\cos\epsilon\sin\phi - \cos\phi\sin\beta\} + \cos\beta\sin\epsilon\cos\theta\right]\end{aligned} \tag{23}$$

The phase $\Phi(t)$ of the received signal is given by

$$\begin{aligned}\Phi(t) &= 2\pi\int_0^t f'(t')dt' \\ &= 2\pi f_o\int_0^t\left[1 + \frac{\mathbf{v}.\mathbf{n}}{c}(t')\right]dt'\end{aligned} \tag{24}$$

Here we assume the initial phase of the wave to be zero. After straight-forward calculation we obtain

$$\begin{aligned}\Phi(t) &= 2\pi f_o\Big[t + \frac{R_{se}}{c}\sin\theta\cos\phi' + \frac{R_e}{c}\sin\alpha\{\sin\theta(\sin\beta\cos\epsilon\sin\phi + \cos\phi\cos\beta) + \\ &\quad \sin\beta\sin\epsilon\cos\theta\} - \frac{R_{se}}{c}\sin\theta\cos\phi - \frac{R_e}{c}\sin\alpha\{\sin\theta(\sin\beta_o\cos\epsilon\sin\phi + \\ &\quad \cos\phi\cos\beta_o) + \sin\beta_o\sin\epsilon\cos\theta\}] \\ &= 2\pi f_o t + \mathcal{Z}\cos(w_{orb}t - \phi) + \mathcal{P}\sin(w_{rot}t) + \mathcal{Q}\cos(w_{rot}t) - \mathcal{R} - \mathcal{Q} \\ &= 2\pi f_o t + \mathcal{Z}\cos(a\xi_{rot} - \phi) + \mathcal{N}\cos(\xi_{rot} - \delta) - \mathcal{R} - \mathcal{Q}\end{aligned} \tag{25}$$

where

$$\left.\begin{aligned}\mathcal{P} &= 2\pi f_o\tfrac{R_e}{c}\sin\alpha(\cos\beta_o(\sin\theta\cos\epsilon\sin\phi + \cos\theta\sin\epsilon) - \sin\beta_o\sin\theta\cos\phi)\,, \\ \mathcal{Q} &= 2\pi f_o\tfrac{R_e}{c}\sin\alpha(\sin\beta_o(\sin\theta\cos\epsilon\sin\phi + \cos\theta\sin\epsilon) + \cos\beta_o\sin\theta\cos\phi)\,, \\ \mathcal{N} &= \sqrt{\mathcal{P}^2 + \mathcal{Q}^2}\,, \\ \mathcal{Z} &= 2\pi f_o\tfrac{R_{se}}{c}\sin\theta\,, \\ \mathcal{R} &= \mathcal{Z}\cos\phi\,,\end{aligned}\right\} \tag{26}$$

$$\left.\begin{aligned} \delta &= \tan^{-1}\frac{\mathcal{P}}{\mathcal{Q}}\,, \\ \phi' &= w_{orb}t-\phi\,, \\ \xi_{orb} &= w_{orb}t \;=\; a\xi_{rot}; \quad a \;=\; w_{orb}/w_{rot} \;\approx\; 1/365.26\,, \\ \xi_{rot} &= w_{rot}t \end{aligned}\right\} \tag{27}$$

The two polarisation states of the signal can be taken as

$$h_+(t) = h_{o_+}\cos[\Phi(t)] \tag{28}$$

$$h_\times(t) = h_{o_\times}\sin[\Phi(t)] \tag{29}$$

h_{o_+}, $h_{o_\times}$ are the time independent amplitude of $h_+(t)$, and $h_\times(t)$ respectively.

To understand the nature of the FM let us consider the function

$$h(t) = \cos[\Phi(t)] \tag{30}$$

and analyse it for one day observation data. The FT is given via

$$\left[\tilde{h}(f)\right]_d = \int_0^T \cos[\Phi(t)]e^{-i2\pi ft}dt\;; \qquad T = \;one\;sidereal\;day\; = 86164\;sec. \tag{31}$$

This splits into two terms as

$$\left[\tilde{h}(f)\right]_d = I_{\nu_-} + I_{\nu_+}\;; \tag{32}$$

$$I_{\nu_-} \;=\; \frac{1}{2w_{rot}}\int_0^{2\pi} e^{i[\xi\nu_- + \mathcal{Z}\cos(a\xi-\phi)+\mathcal{N}\cos(\xi-\delta)-\mathcal{R}-\mathcal{Q}]}d\xi\,, \tag{33}$$

$$I_{\nu_+} \;=\; \frac{1}{2w_{rot}}\int_0^{2\pi} e^{-i[\xi\nu_+ + \mathcal{Z}\cos(a\xi-\phi)+\mathcal{N}\cos(\xi-\delta)-\mathcal{R}-\mathcal{Q}]}d\xi\,, \tag{34}$$

$$\nu_\mp \;=\; \frac{f_o \mp f}{f_{rot}}; \quad \xi \;=\; \xi_{rot} \;=\; w_{rot}t \tag{35}$$

Numerical result shows that I_{ν_+} oscillates very fast and contributes very little to $\left[\tilde{h}(f)\right]_d$. Hence, hereafter, we drop I_{ν_+} from Eq. (32) and write ν in place of ν_-. Using the identity

$$e^{\pm i\kappa\cos\vartheta} = J_o(\pm\kappa) + 2\sum_{l=1}^{l=\infty} i^l J_l(\pm\kappa)\cos l\vartheta \tag{36}$$

we obtain

$$\left[\tilde{h}(f)\right]_d \simeq \frac{1}{2w_{rot}} e^{i(-\mathcal{R}-\mathcal{Q})} \int_0^{2\pi} e^{i\nu\xi} \left[J_o(\mathcal{Z}) + 2\sum_{k=1}^{k=\infty} J_k(\mathcal{Z}) i^k \cos k(a\xi - \phi)\right] \times \left[J_o(\mathcal{N}) + 2\sum_{m=1}^{m=\infty} J_m(\mathcal{N}) i^m \cos m(\xi - \delta)\right] d\xi \quad (37)$$

where J stands for the Bessel function of the first kind. After performing the integration we get

$$\left[\tilde{h}(f)\right]_d \simeq \frac{\nu}{2w_{rot}} \sum_{k=-\infty}^{k=\infty} \sum_{m=-\infty}^{m=\infty} e^{i\mathcal{A}} \mathcal{B}[\mathcal{C} - i\mathcal{D}] \; ; \quad (38)$$

$$\left.\begin{aligned} \mathcal{A} &= \tfrac{(k+m)\pi}{2} - \mathcal{R} - \mathcal{Q} \\ \mathcal{B} &= \tfrac{J_k(\mathcal{Z}) J_m(\mathcal{N})}{\nu^2 - (ak+m)^2} \\ \mathcal{C} &= \sin 2\nu\pi \cos(2ak\pi - k\phi - m\delta) - \tfrac{ak+m}{\nu}\{\cos 2\nu\pi \sin(2ak\pi - k\phi - m\delta) + \\ &\quad \sin(k\phi + m\delta)\} \\ \mathcal{D} &= \cos 2\nu\pi \cos(2ak\pi - k\phi - m\delta) + \tfrac{ka+m}{\nu} \sin 2\nu\pi \sin(2ak\pi - k\phi - m\delta) - \\ &\quad \cos(k\phi + m\delta) \end{aligned}\right\} \quad (39)$$

The FT of the two polarisation states of the wave can now be written as

$$\begin{aligned} \left[\tilde{h}_+(f)\right]_d &= h_{o_+} \left[\tilde{h}(f)\right]_d \\ &\simeq \frac{\nu h_{o_+}}{2w_{rot}} \sum_{k=-\infty}^{k=\infty} \sum_{m=-\infty}^{m=\infty} e^{i\mathcal{A}} \mathcal{B}[\mathcal{C} - i\mathcal{D}] \; ; \end{aligned} \quad (40)$$

$$\begin{aligned} \left[\tilde{h}_\times(f)\right]_d &= -ih_{o_\times} \left[\tilde{h}(f)\right]_d \\ &\simeq \frac{\nu h_{o_\times}}{2w_{rot}} \sum_{k=-\infty}^{k=\infty} \sum_{m=-\infty}^{m=\infty} e^{i\mathcal{A}} \mathcal{B}[\mathcal{D} - i\mathcal{C}] \end{aligned} \quad (41)$$

The FT of the FM signal contains the double series Bessel functions. The Bessel functions have contributions due to the rotational as well as the orbital motion of the earth. It is remarked that Jotania et al. (1996) have analysed FT of FM signal for one day observation time. They have taken specific detector as well as source location. They have also neglected the orbital motion. Our analysis generalizes their results. We may now compute $\left[\tilde{h}(f)\right]_d$

and may plot its behaviour. To achieve this we have made use of *Mathematica* software. We know that the value of Bessel function decreases rapidly as its order exceed the argument. Accordingly, one computes in practice only a finite number of terms in the above infinite series. Figure (1) represents such a plot for

$$\left.\begin{array}{lll} f_o = 80\ Hz\,, & h_{o_+} = h_{o_\times} = 1 & \\ \alpha = \pi/3\,, & \beta_o = \pi/4\,, & \gamma = 2\pi/5\,, \\ \theta = \pi/36\,, & \phi = \pi\,, & \psi = \pi/6. \end{array}\right\} \tag{42}$$

with a resolution equal to $1/T_o = 1.16 \times 10^{-5}$ Hz. For the present case we found it sufficient to evaluate the infinite series for $k = -21900$ to $+21900$ and $m = -10$ to $+10$. Figures (2) and (3) represent the plot of the FT at resolution 10^{-6} Hz and 10^{-7} Hz. A careful look at these plots reveals that the resolution of Fig. (1) does not represent the details of the dominant peaks around f_o, whereas, Fig. (3) does not give any new behaviour as compared to Fig. (2). Hence, we may say that a resolution of about 10^{-6} Hz is required to understand the correct behaviour of the FT for one day observation data. In this reference let us recall that the data analysis for Fast Fourier Transform (FFT) limits the resolution to $1/T_o$. However, the detector output may provide us higher resolution. Thus the semi-analytical analysis presented here may provide more information as compared to FFT.

4 Fourier transform of the complete response

The complete response $R(t)$, in view of Eqs. (5), (14), (15), (28) and (29) may be written as

$$R(t) = R_+(t) + R_\times(t)\ ; \tag{43}$$

$$R_+(t) = h_{o_+}\left[F_{1_+}\cos 2\beta + F_{2_+}\sin 2\beta + F_{3_+}\cos\beta + F_{4_+}\sin\beta + F_{5_+}\right]\cos[\Phi(t)]\,, \tag{44}$$

$$R_\times(t) = h_{o_\times}\left[F_{1_\times}\cos 2\beta + F_{2_\times}\sin 2\beta + F_{3_\times}\cos\beta + F_{4_\times}\sin\beta + F_{5_\times}\right]\sin[\Phi(t)] \tag{45}$$

Here, for simplicity, we have taken the angle between the arms of the detector equal to $\pi/2$ i.e. $\Omega = \pi/4$. Now the FT of the complete response may be expressed as

$$\tilde{R}(f) = \tilde{R}_+(f) + \tilde{R}_\times(f) \tag{46}$$

Substituting β as given by (22) one obtains

$$\begin{aligned} R_+(t) = \frac{h_{o_+}}{2}\Big[&e^{-i2\beta_o}(F_{1_+} + iF_{2_+})e^{-i2w_{rot}t} + e^{i2\beta_o}(F_{1_+} - iF_{2_+})e^{i2w_{rot}t} + \\ &e^{-i\beta_o}(F_{3_+} + iF_{4_+})e^{-iw_{rot}t} + e^{i\beta_o}(F_{3_+} - iF_{4_+})e^{iw_{rot}t} + 2F_{5_+}\Big]\cos[\Phi(t)] \end{aligned} \tag{47}$$

and similar expression for $R_\times(t)$. Now it is straight-forward to obtain the expressions for $\tilde{R}_+(f)$ and $\tilde{R}_\times(f)$ as

$$\begin{aligned}\left[\tilde{R}_+(f)\right]_d &= \frac{h_{o_+}}{2}\left[e^{-i2\beta_o}(F_{1_+}+iF_{2_+})\left[\tilde{h}(f+2f_{rot})\right]_d + e^{i2\beta_o}(F_{1_+}-iF_{2_+})\left[\tilde{h}(f-2f_{rot})\right]_d\right. \\ &+ e^{-i\beta_o}(F_{3_+}+iF_{4_+})\left[\tilde{h}(f+f_{rot})\right]_d + e^{i\beta_o}(F_{3_+}-iF_{4_+})\left[\tilde{h}(f-f_{rot})\right]_d \\ &\left.+ 2F_{5_+}\left[\tilde{h}(f)\right]_d\right]\ ; \end{aligned} \tag{48}$$

$$\begin{aligned}\left[\tilde{R}_\times(f)\right]_d &= \frac{h_{o_\times}}{2}\left[e^{-i2\beta_o}(F_{2_\times}-iF_{1_\times})\left[\tilde{h}(f+2f_{rot})\right]_d - e^{i2\beta_o}(F_{2_\times}+iF_{1_\times})\left[\tilde{h}(f-2f_{rot})\right]_d\right. \\ &+ e^{-i\beta_o}(F_{4_\times}-iF_{3_\times})\left[\tilde{h}(f+f_{rot})\right]_d - e^{i\beta_o}(F_{4_\times}+iF_{3_\times})\left[\tilde{h}(f-f_{rot})\right]_d \\ &\left.- i2F_{5_\times}\left[\tilde{h}(f)\right]_d\right] \end{aligned} \tag{49}$$

Collecting our results the FT of the complete response of the detector for one day time integration will be

$$\begin{aligned}\left[\tilde{R}(f)\right]_d &= \frac{1}{2}\left[e^{-i2\beta_o}\left[\tilde{h}(f+2f_{rot})\right]_d\left[h_{o_+}(F_{1_+}+iF_{2_+})+h_{o_\times}(F_{2_\times}-iF_{1_\times})\right]+\right. \\ &e^{i2\beta_o}\left[\tilde{h}(f-2f_{rot})\right]_d\left[h_{o_+}(F_{1_+}-iF_{2_+})-h_{o_\times}(F_{2_\times}+iF_{1_\times})\right]+ \\ &e^{-i\beta_o}\left[\tilde{h}(f+f_{rot})\right]_d\left[h_{o_+}(F_{3_+}+iF_{4_+})+h_{o_\times}(F_{4_\times}-iF_{3_\times})\right]+ \\ &e^{i\beta_o}\left[\tilde{h}(f-f_{rot})\right]_d\left[h_{o_+}(F_{3_+}-iF_{4_+})-h_{o_\times}(F_{4_\times}+iF_{3_\times})\right]+ \\ &\left.2\left[\tilde{h}(f)\right]_d\left[h_{o_+}F_{5_+}-ih_{o_\times}F_{5_\times}\right]\right] \end{aligned} \tag{50}$$

This shows that due to AM every Doppler modulated FM signal will split in four additional lines at $f \pm 2f_{rot}$ and $f \pm f_{rot}$, where f_{rot} is the rotational frequency of Earth ($f_{rot} \approx 1.16 \times 10^{-5}$ Hz).

We have plotted in Fig. (4) the power spectrum of the noise free complete response of the signal for its various parameters as given by (42). The contribution in the power spectrum of the modulation at frequencies $f + 2f_{rot}$, $f - 2f_{rot}$, $f + f_{rot}$ and $f - f_{rot}$ and f are represented respectively in Figs. (5), (6), (7), (8) and (9). It is observed that the most of the power will be at $f + 2f_{rot}$ and least power will be in $f - f_{rot}$.

5 Conclusion

In this paper we have considered the effect of earth's motion on the response of the detector through FT analysis. It can be easily inferred from Eqs. (50) and (40, 41) that the splitting of frequencies (i) in AM arises explicitly due to rotational motion and (ii) in FM arises due to rotational as well as orbital motion of the earth. In view of the fact that the data output at the detector is available in discrete form, the analytical FT is not very convenient and one normally employs the popular FFT. However, FFT has resolution limited to $1/T_o$. Further, it is important to understand for how much time one can ignore the frequency shift arising due to Doppler effect. In fact, Schutz (1991) has demonstrated that these effects due to rotational motion are important after the time given by

$$T_{max} = \left(\frac{2c}{\omega_{rot}^2 f_o R_e}\right)^{1/2} \simeq 70 \left(\frac{f_o}{1kHz}\right)^{-1/2} min. \tag{51}$$

This means that for GW signal for frequency 80 Hz one has to take into account these effects after data time $\simeq$ 4 hours. The analytical FT studied in this paper leads to following inferences:

(i) FFT for one day observation data will not provide sufficient resolution as to represent the correct picture of the frequency splitting.

(ii) The adequate resolution required for one day observation $\simeq 10^{-6}$ Hz.

(iii) The frequency split due to FM for frequency $f_o = 80$ Hz and source at (θ, ϕ) = $(\pi/36, \pi)$ is $\simeq 2 \times 10^{-4}$ Hz and due to AM is $\simeq 4.64 \times 10^{-5}$ Hz.

(iv) The drop in amplitude due to FM alone is about 56%

(v) The drop in amplitude due to AM alone is about 18%.

(vi) The drop in amplitude for the complete response is about 74%.

(vii) The maximum power due to AM is associated with $f_o + 2f_{rot}$.

It is remarked that the drop of the amplitude in complete response is severe both due to AM and FM as the relevant frequency range lies in the same region.

We have presented the FT analysis assuming the phase of the GW to be zero at that instant $t = 0$. However, one may relax this condition and may obtain the results easily by taking into consideration the effects of change of the time origin.

Acknowledgments

The authors are thankful to Prof. S. Dhurandhar, IUCAA, Pune and Dr. S.S. Prasad, UNPG college, Padrauna for stimulating discussions. The authors are extremely thankful to the anonymous referee for his hardwork in pinpointing the errors and making the detailed suggestions which resulted in the improvement of the paper. The authors are also thankful to IUCAA for providing hospitality where major part of the work was carried out. This work is supported through research scheme vide grant number SP/S2/0-15/93 by DST, New Delhi.

References

[1] Brady, P.R. and Creighton, 2000, Phys. Rev. D , 61, 082001.

[2] Brady, P.R., et al., 1998, Phys. Rev. D , 57, 2101.

[3] Goldstein, H., 1980, Classical Mechanics. Addison-wesley, New York.

[4] Jaranowski, P., et al, 1998, Phys. Rev. D , 58, 63001.

[5] Jaranowski, P. and Królak, A., 1999, Phys. Rev. D , 59, 63003.

[6] Jaranowski, P. and Królak, A., 2000, Phys. Rev. D , 61, 62001.

[7] Jotania, K., 1994, Some Aspects of Gravitational Waves Signal Analysis from Coalescing Binaries and Pulsars, Ph.D. thesis, University of Pune, India, unpublished.

[8] Jotania, K. and Dhurandhar, S.V., 1994, Bull. Astron. Soc. India, 22, 303.

[9] Jotania et al., 1996, Astronomy and Astrophysics, 306, 317-325.

[10] Królak, A., Preprint gr-qc/9903099 (1999).

[11] Schutz, B.F., and Tinto, M., 1987, MNRAS, 224, 131.

[12] Schutz, B.F., 1991, in The Detection of Gravitational Waves. ed. Blair, D.G., Cambridge University Press, Cambridge, England.

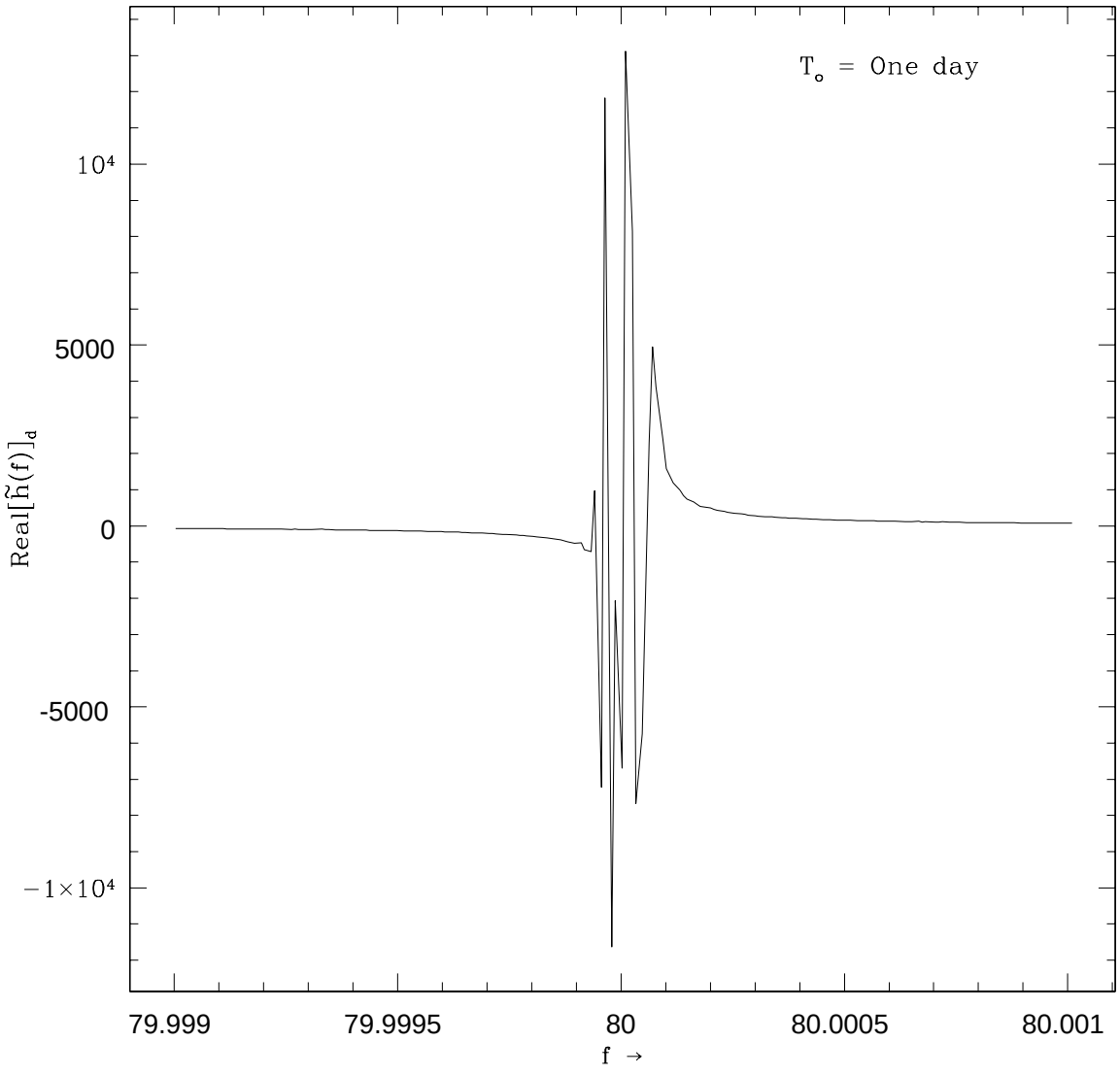

Figure 1: FT of a FM signal frequency, $f_o = 80$ Hz, from a source located at $(\pi/36, \pi)$ with a resolution of 1.16×10^{-5} Hz

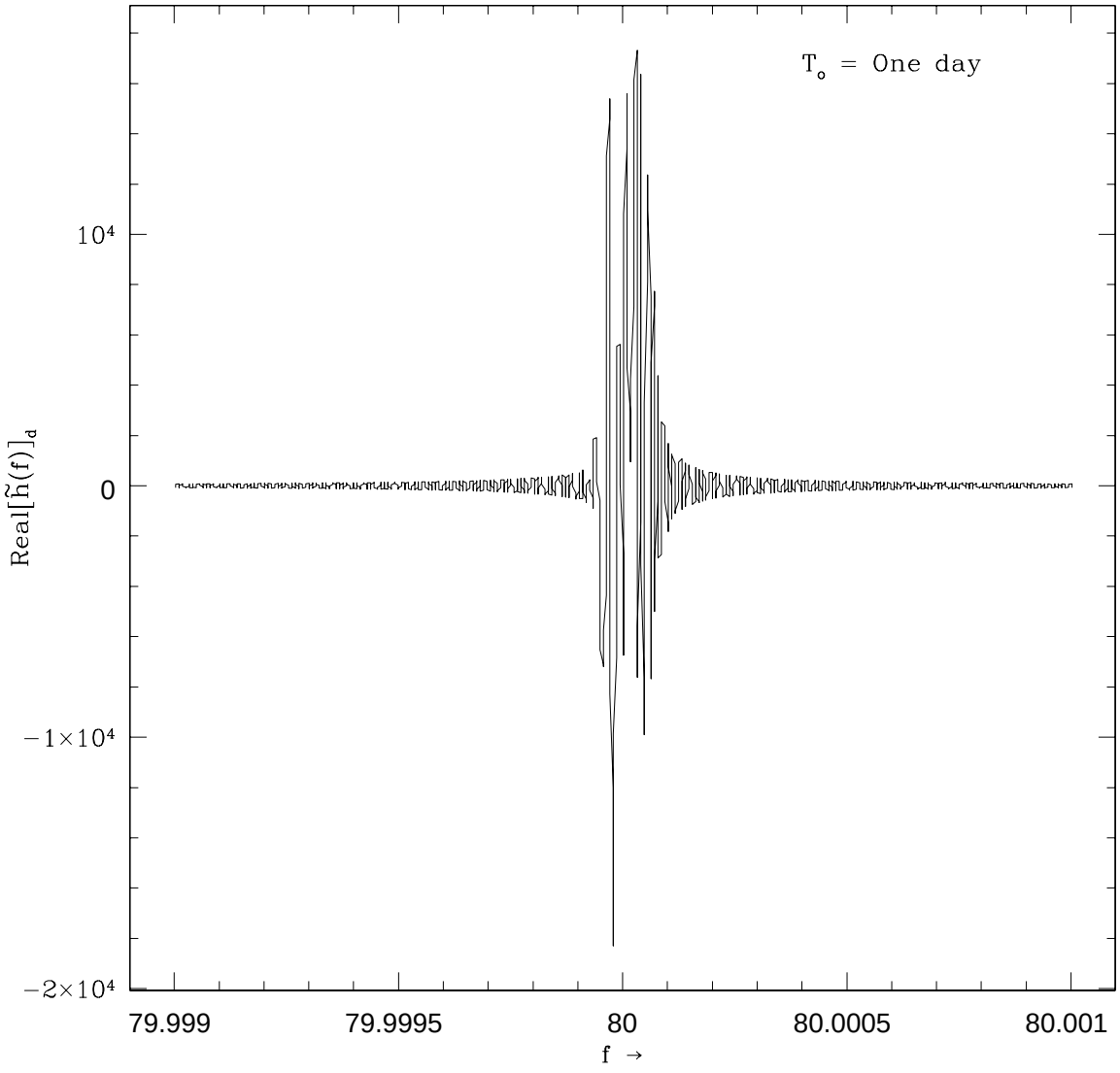

Figure 2: FT of a FM signal frequency, $f_o = 80$ Hz, from a source located at $(\pi/36, \pi)$ with a resolution of 10^{-6} Hz

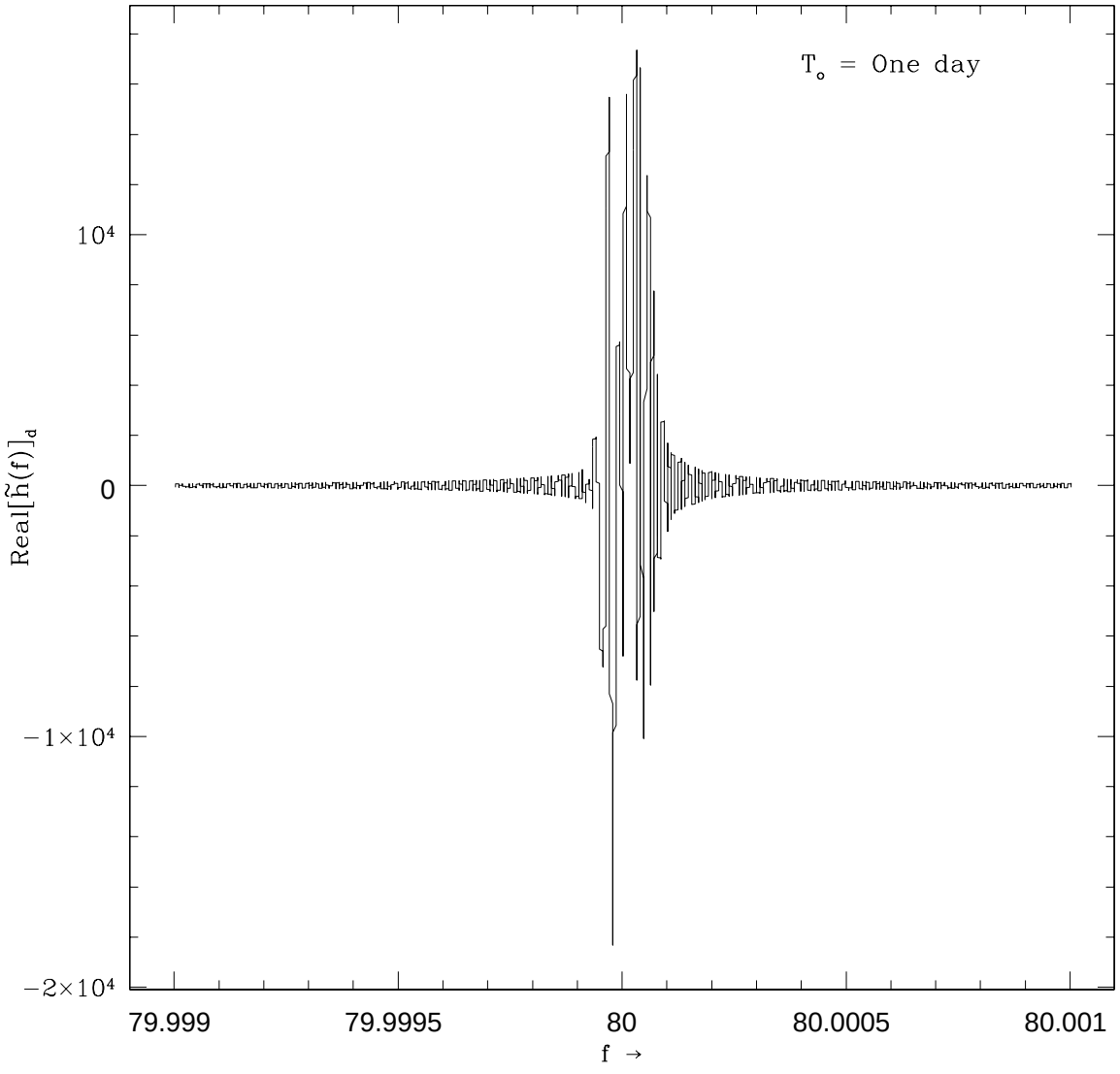

Figure 3: FT of a FM signal frequency, $f_o = 80$ Hz, from a source located at $(\pi/36, \pi)$ with a resolution of 10^{-7} Hz

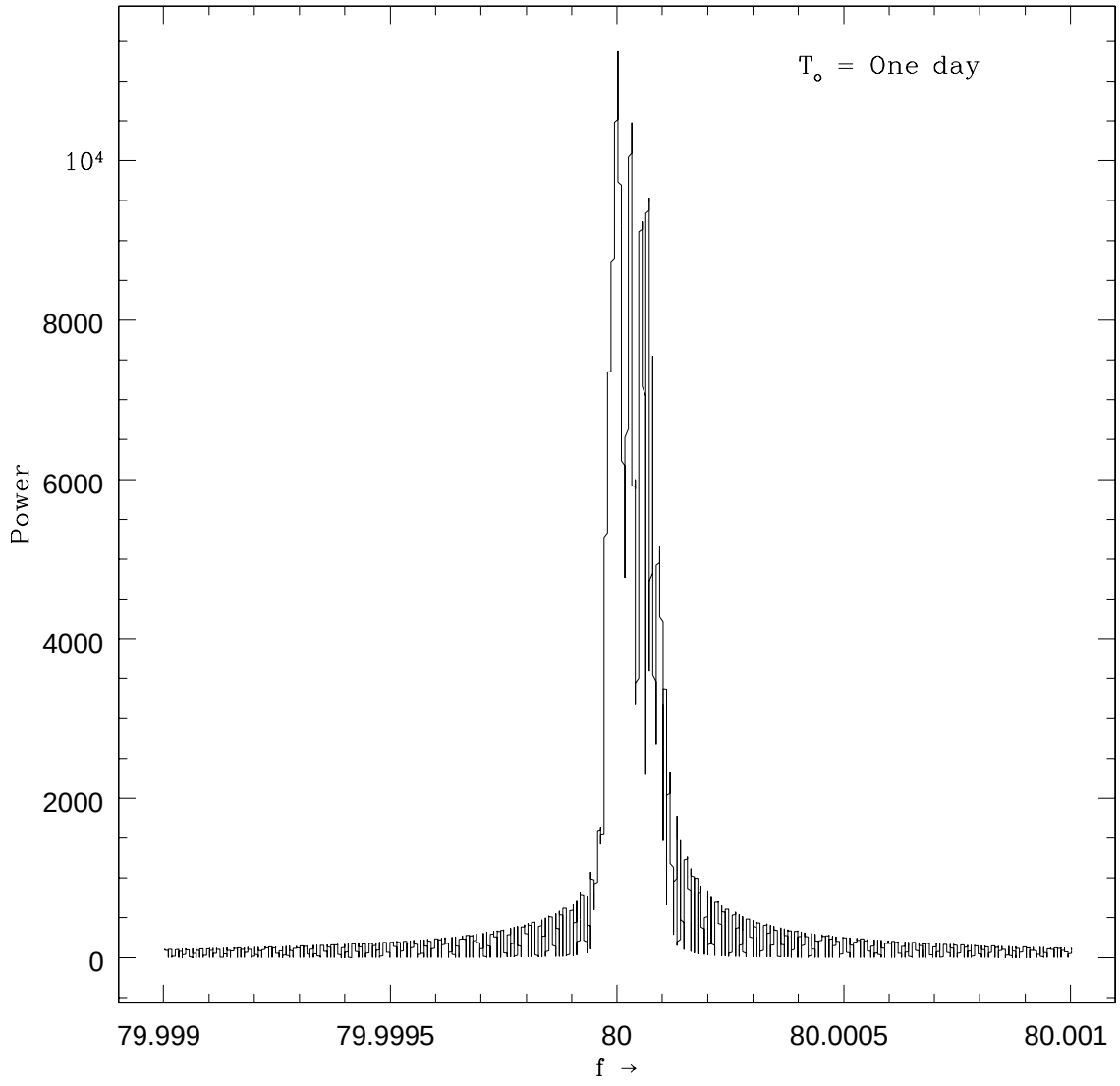

Figure 4: Power spectrum of the complete response of a Doppler modulated signal frequency, $f_o = 80$ Hz, from a source located at $(\pi/36, \pi)$ with a resolution of 10^{-7} Hz

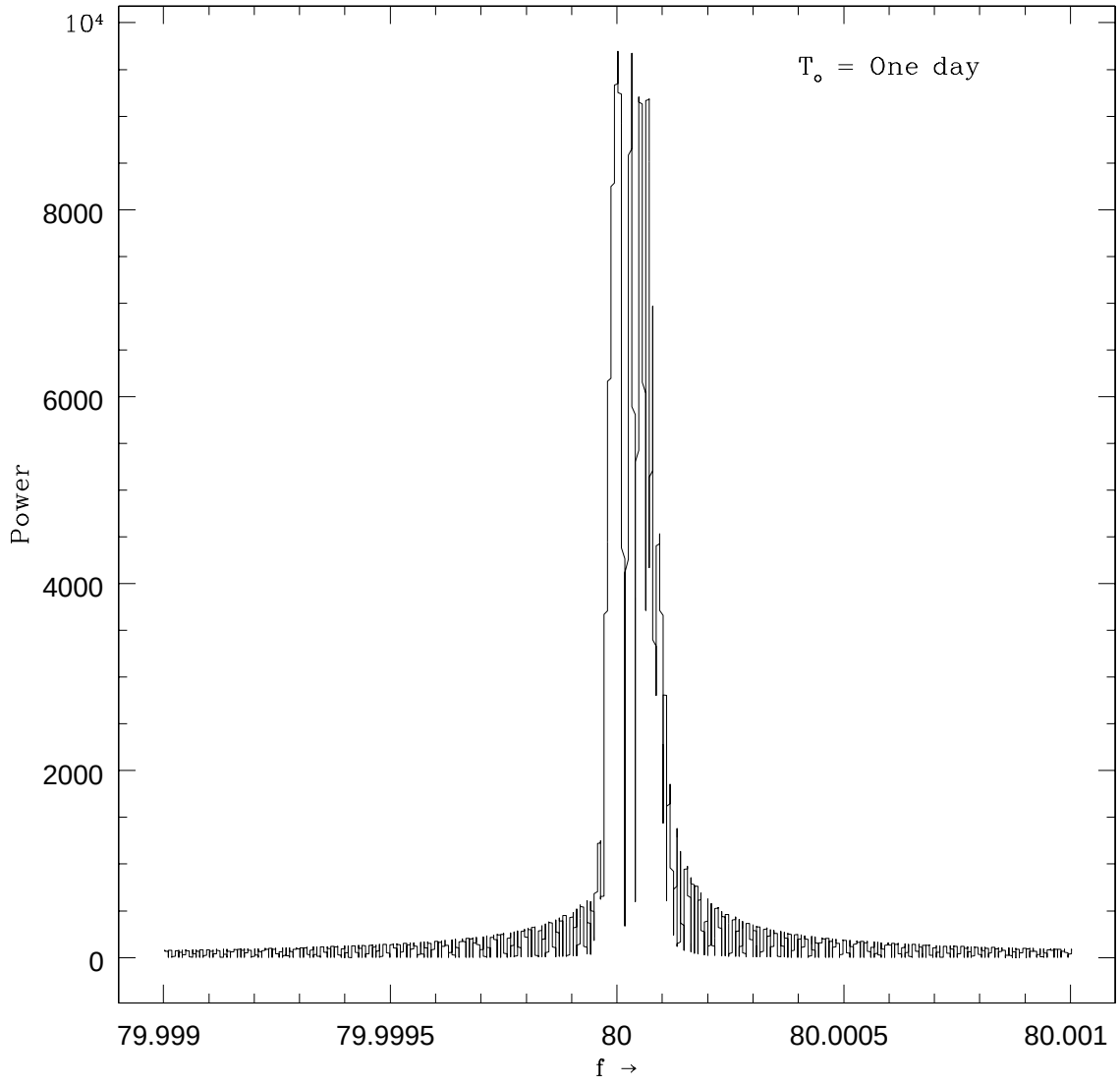

Figure 5: Power spectrum of a Doppler modulated signal at frequencies $f + 2f_{rot}$ of signal frequency, $f_o = 80$ Hz, from a source located at $(\pi/36, \pi)$ with a resolution of 10^{-7} Hz

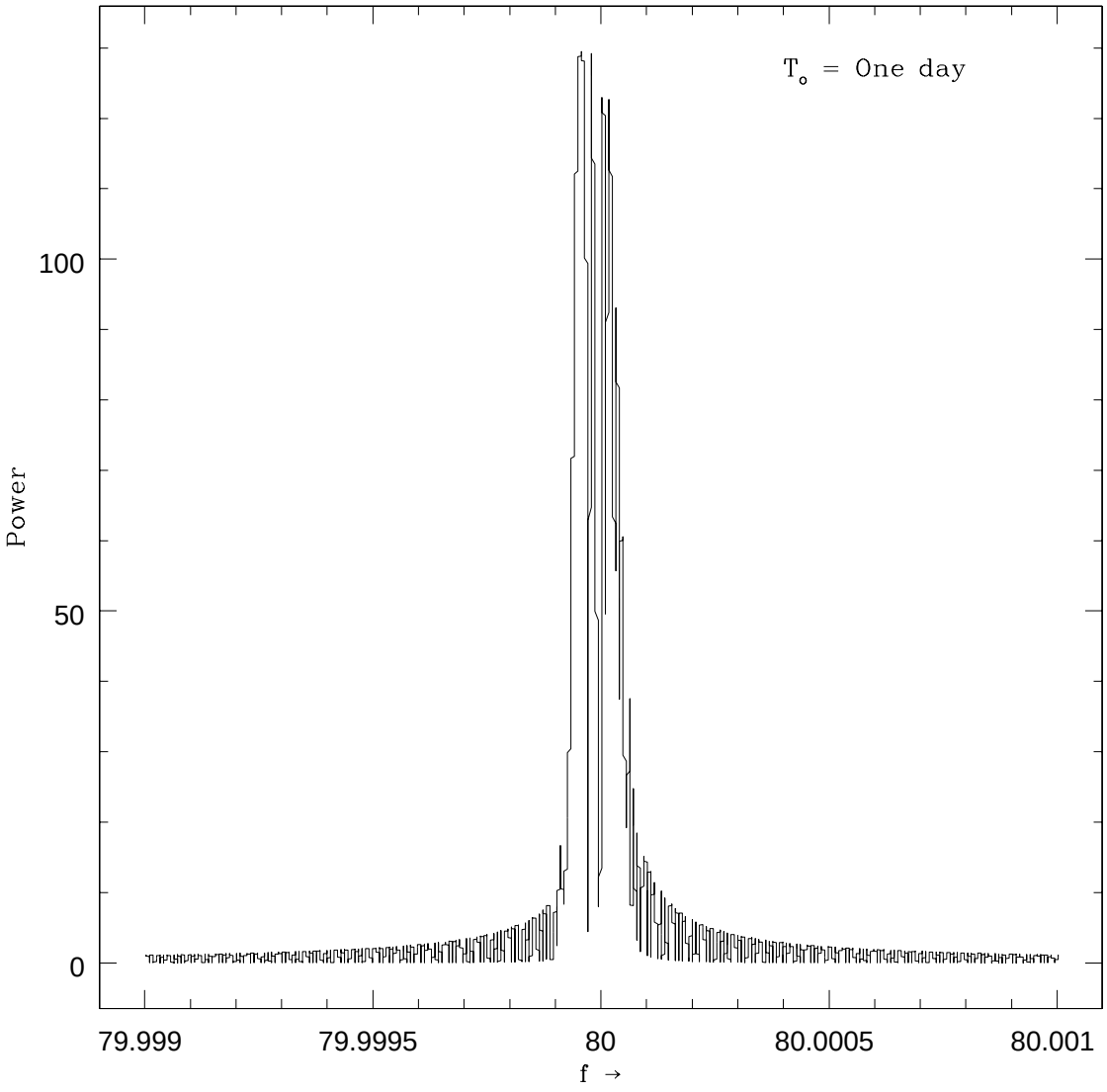

Figure 6: Power spectrum of a Doppler modulated signal at frequencies $f - 2f_{rot}$ of signal frequency, $f_o = 80$ Hz, from a source located at $(\pi/36, \pi)$ with a resolution of 10^{-7} Hz

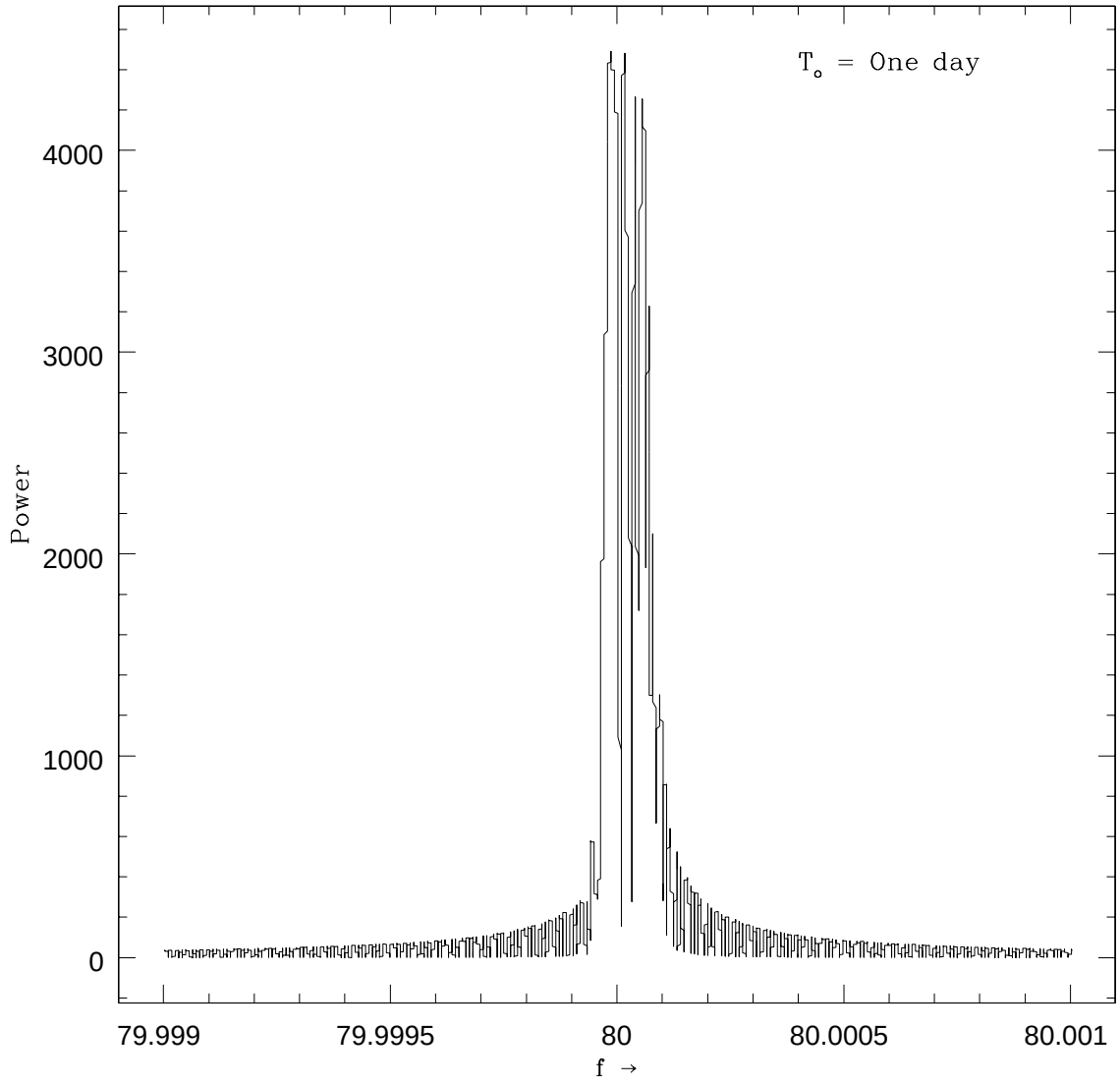

Figure 7: Power spectrum of a Doppler modulated signal at frequencies $f + f_{rot}$ of signal frequency, $f_o = 80$ Hz, from a source located at $(\pi/36, \pi)$ with a resolution of 10^{-7} Hz

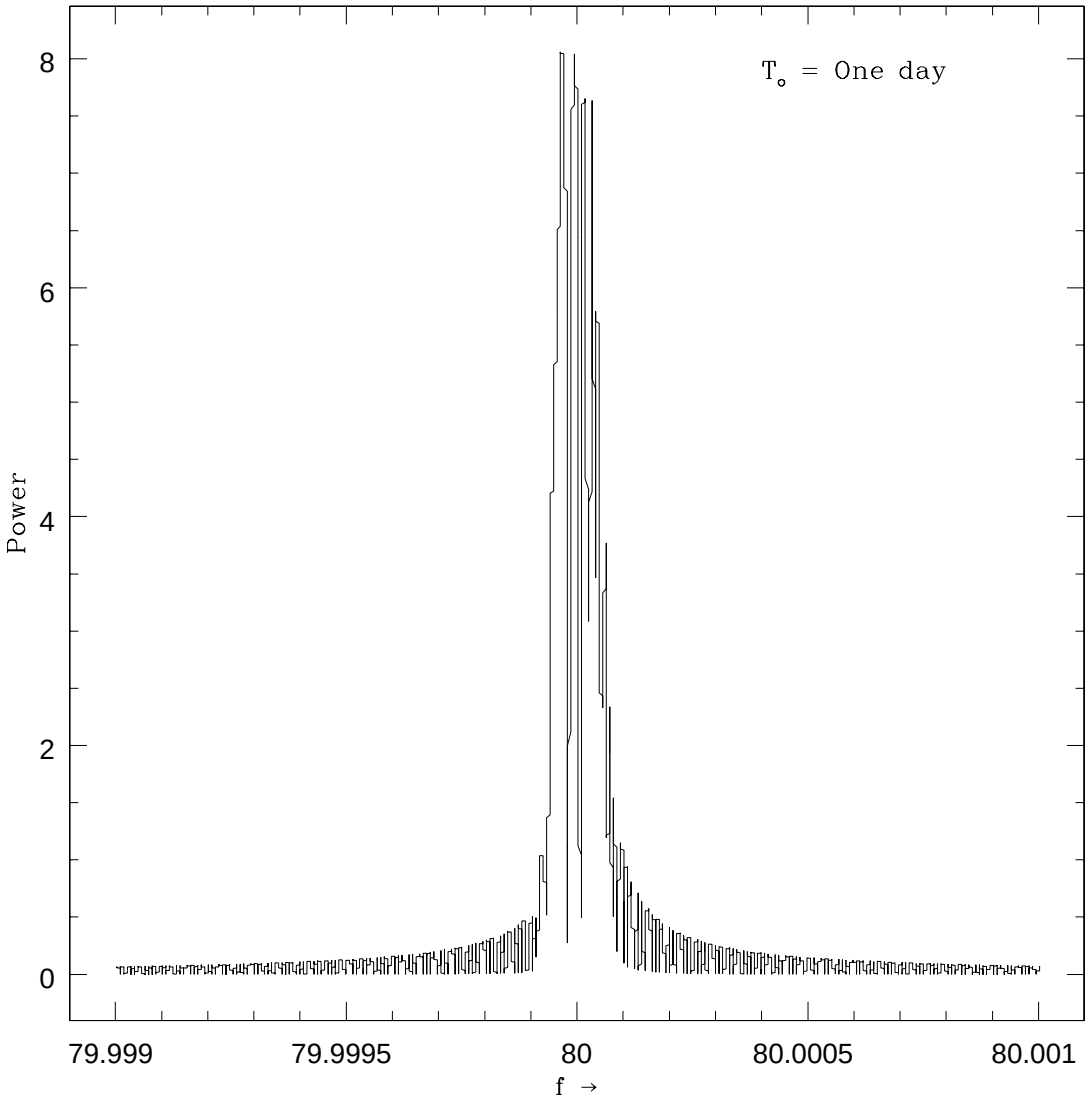

Figure 8: Power spectrum of a Doppler modulated signal at frequencies $f - f_{rot}$ of signal frequency, $f_o = 80$ Hz, from a source located at $(\pi/36, \pi)$ with a resolution of 10^{-7} Hz

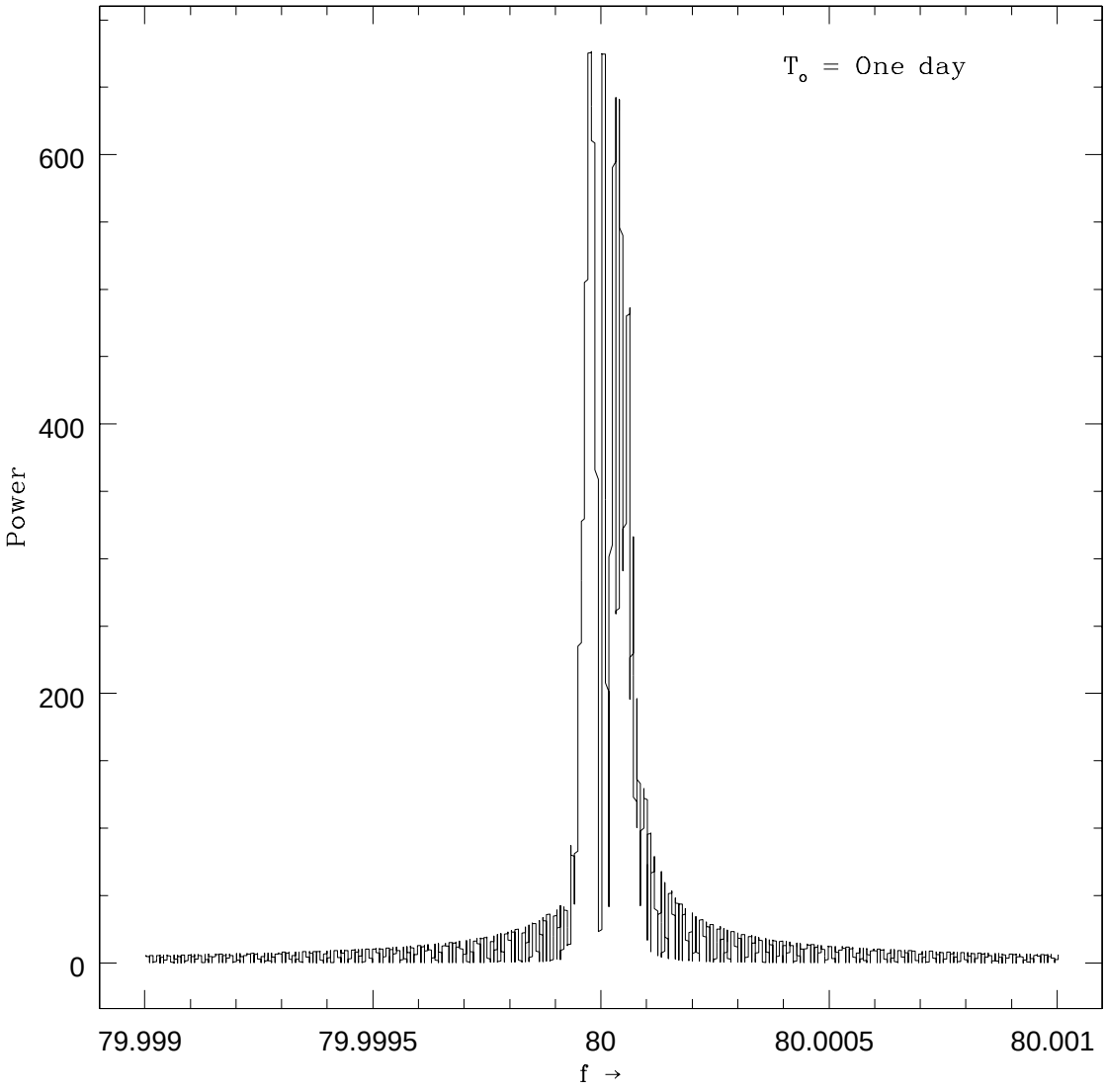

Figure 9: Power spectrum of a Doppler modulated signal at frequencies f of signal frequency, $f_o = 80$ Hz, from a source located at $(\pi/36, \pi)$ with a resolution of 10^{-7} Hz